RSC Advances

PAPER

View Article Online
View Journal | View Issue

Cite this: *RSC Adv.*, 2021, **11**, 20737

Revisiting the valence stability and preparation of perovskite structure type oxides ABO_3 with the use of Madelung electrostatic potential energy and lattice site potential

Masahiro Yoshimura †*[a] and Kripasindhu Sardar[b]

Valence stability of aliovalent ions is mostly correlated with lattice site potential in ionic crystals. Madelung electrostatic potential is obtained by adding all the lattice site potentials for all the ions present in a crystal structure. Therefore, valence stability and the stability of a crystal structure can be better understood with consideration of both the lattice site potential and Madelung electrostatic potential. This was first demonstrated more than four decades ago by one of the present authors. We revisit this situation by using re-calculated lattice site potential and Madelung electrostatic potential for perovskite structure type ABO_3 compounds using a new computer program VESTA. We show that the formation of a perovskite structure type compound with the general formula ABO_3 (where A and B are cations and O is an oxide ion) becomes energetically favorable when it has a higher Madelung electrostatic potential than the combined Madelung electrostatic potential of parent binary compounds AO and B_2O_3 or BO_2. It is further shown that strong lattice site potential results in stability of high valence or high valence ions can be stabilized in a lattice site with strong lattice-site potential. It further follows that certain ions experience maximum lattice site potential at the B ion lattice site of the perovskite structure when compared to other structures such as fluorite BO_2, rutile BO_2 and corundum B_2O_3. Therefore, (i) the stability of an ion with a high (and uncommon) valence state at the B site being higher than that at the A site, (ii) occurrence of point defects at A or O sites with weak lattice site potentials, respectively and (iii) instability of perovskite $A^{4+}B^{2+}O_3$, and $A^{5+}B^{1+}O_3$ compounds, respectively can be rationalized by lattice site potential and Madelung electrostatic potential analysis.

Received 12th March 2021
Accepted 3rd May 2021

DOI: 10.1039/d1ra01979a

rsc.li/rsc-advances

Introduction

An enormous number of solids show crystallographic structural similarity to the mineral perovskite ($CaTiO_3$) and have the general formula ABX_3. Metal oxides with chemical formula ABO_3 are a subclass of this large family of compounds. For many years, perovskite oxides have been studied extensively in the literature of chemistry, physics and geology for a large variety of solid state phenomena associated with electric, optical, thermal and magnetic properties. A large number of oxides with perovskite type structures are possible to synthesise in a laboratory for applications in vast areas spanning from electronics to catalysis. It is of immense importance to understand the factors that may correlate with the formation and stability of perovskite structure type ABO_3 compounds for the design of new compounds with novel structures containing desired valence states of B cations.

The reason for why many compounds would take perovskite structure type ABX_3 had been explained from ion-packing & tolerance factor, by Goldschmidt in 1926.[1] Even now, most of the research articles and text books on the assessment of stability of perovskite structure type ABO_3 oxides focus on the geometric parameters such as tolerance factor, and structure-field map.[2–5] However, lattice and valence stabilities should be more related to thermodynamic energy and originate from thermodynamic principles rather than numerical geometrical parameters. Crystal chemistry and thermodynamic energy of ionic solids are reflected into Madelung electrostatic potential as shown by Van Gool and Piken in 1969.[6,7] "The valence stability using lattice site-potential" of perovskite structure type ABO_3 was demonstrated by one of the authors of this article (M. Yoshimura) and was considered for the first time in 1974.[8] This was referred by Rustam Roy in 1975 in a plenary lecture presented as the Robert B. Sosman Memorial Lecture at the 77th annual meeting of the American ceramics society and was

[a]*Tokyo Institute of Technology, Tokyo, Japan. E-mail: yoshimur@ncku.edu.tw*
[b]*Department of Material Science and Engineering, National Cheng Kung University, Tainan, 701, Taiwan*

† Present address: Hierarchical Green-Energy Materials (Hi-GEM) Research Center and NCKU 90 and beyond project, Distinguished Visiting Chair Professor, Department of Materials Science and Engineering, National Cheng Kung University, Tainan, Taiwan, 701

published in 1977.[9] This is a novel and very less explored concept. We also note that not many researchers have been able to consider this concept perhaps due to the inaccessibility of the original article.[8] Here, the present article is written by re-visiting Madelung lattice energy and site potentials based upon recent data calculated using VESTA[10] program and recent crystallographic (structural) and thermodynamic data. We emphasize on the fact that ionic solids are stabilized due to the gain in lattice energy that is reflected in Madelung electrostatic potential (E_M). Nevertheless, recently, Hoppe demonstrated that the enthalpy of formation of solids is reflected in Madelung electrostatic potential in 1995[11] and Glasser has shown that for ionic solids the lattice energy and Madelung electrostatic potential energy (E_M) has a linear relationship in 2012.[12]

The ideal perovskite structure type of ABO_3 compound has a cubic unit cell. This structure can be constructed from corner shared BO_6 octahedra with A cation being present at the 12 coordinated interstitial position within the octahedral network (Fig. 1a). A and B cations are coordinated by 12 and six O^{2-} ions, respectively and O^{2-} ion is coordinated by four A and two B cations. Several structural modification of cubic perovskite structure has been identified such as tetragonal, orthorhombic, rhombohedral, hexagonal, and monoclinic, respectively either as polymorph of ABO_3 or upon chemical modification. The most important chemical fact of ABO_3 perovskite compound is that, apart from noble gasses and nonmetals, A or B in ABO_3 can be chosen from almost all elements and several aliovalent A or B ions such as $A_{1-x}A'_x$ or $B_{1-y}B'_y$, respectively can be combined in a single compound. Furthermore, non-ideal stoichiometry of oxygen or A such as ABO_{3-z} or $A_{1-x}BO_3$, respectively are regularly observed. It is further interesting that many BO_3 compounds can adopt perovskite type structure where A cation is completely absent for example ReO_3. Therefore, the structural skeleton formation by BO_3 sub lattice is generally regarded as prerequisite for the formation of perovskite structure type compounds.[2] Furthermore, the BO_3 sub lattice skeleton is primarily stabilized by the electrostatic potential energy gain by ionic arrangements in solid phase and additional stability of perovskite type ABO_3 compounds can arise from (i) the presence of large A cation within the interstitial position, (ii) crystal field splitting and (iii) hybridization of orbitals.[2]

The total internal energy of ionic solids may be expressed as

$$E = E_M + E_N \quad (1)$$

where E_M is Madelung electrostatic potential energy and E_N is combination of all other energies (repulsive, zero point, crystal field stabilization, vibrational, van der Waals and covalent, energies respectively).[13]

The analysis of Madelung electrostatic potential and lattice site potential of a large number ABO_3 compounds (with varying combination of A and B) led to a set of fundamental criteria for the formation of perovskite structure type ABO_3 with varying combination and valence states of A and B and summarized by Yoshimura *et al.*[8,14] as follows: oxides of A can be reacted with oxides of B to form perovskite structure type ABO_3 compounds if: (i) B ion is smaller than A ion, (ii) valence of B ion is larger or equal to A ion and (iii) sum of valence of A and B ion is six (including mixed valence situation $A'_{1-x}A''_x$ or $B'_{1-y}B''_y$). An in depth analysis showed that the valence stability originates from gain of lattice site potential. Recently, there have been some excellent research work reported in the literature based on the use of Madelung electrostatic potentials energy for understanding the stability of perovskite structure type compounds. Shan *et al.* investigated Li ion insertion in perovskite structure type $SrVO_{3-\delta}$, $La_{2/3}TiO_{3-\delta}$ and (La, Li)$TiO_{3-\delta}$, from the lattice site potential analysis and found that the insertion of lithium ion is limited by the effect of lattice site potential on the valence stability of V and Ti.[15] In these perovskite structure type oxides, the valence state of tetravalent V and Ti can be reduced to 3 upon insertion of monovalent Li ion at an interstitial site. It is interesting to note that for spinel structure type $LiMn_2O_4$ compounds, Ragavendran *et al.* have shown that the Madelung electrostatic potential of $Li_xMn_2O_4$ almost linearly correlates with x and therefore voltage of Li-ion battery made using $LiMn_2O_4$ can be easily estimated from the Madelung

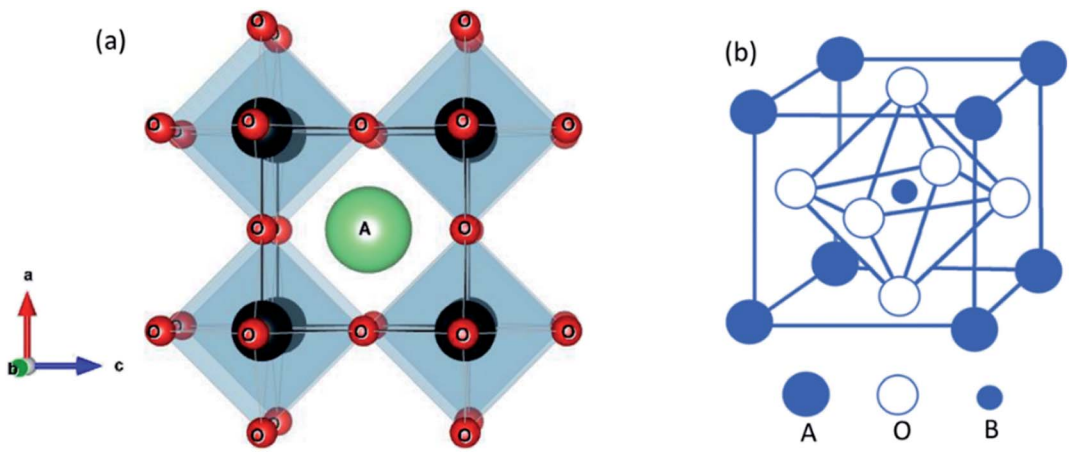

Fig. 1 Ideal cubic perovskite structure of ABO_3 (a) showing corner shared BO_6 octahedra and A cation at the interstitial position and (b) showing B cation and BO_6 octahedra at the center of the unit cell.

electrostatic potential.[16] Furthermore, the perovskite structure-type is not limited to ABO_3 and a large number of organic–inorganic halide crystallise into perovskite type structure with general formula ABX_3. A bottle neck for the realization of full potential of so called 'perovskite solar cells' and related electronic devices has been the degradation of electronic devices fabricated using hybrid organic–inorganic ABX_3 compounds.[17] The degradation of these devices arise from instability of the perovskite structure type hybrid compounds and can also be understood from Madelung electrostatic potential analysis.[18] Furthermore, it has also been shown that the stability of oxides such as Li_4SiO_4 towards the reaction $Li_4SiO_4 + CO_2 \rightarrow Li_2SiO_3 + Li_2CO_3$ has direct consequence on the CO_2 capture and storage abilities and recent study by Oh-ishi *et al.* had successfully employed lattice site potentials analysis of all Li^+ ions in the unit cells of Li_4SiO_4, Li_2SiO_3, and Li_2CO_3 to evaluate the extraordinary stability.[19]

On the other hand, lattice site potential can be used for the estimation of the oxygen to metal charge transfer and bandgap of perovskite type ABO_3 oxides using an ionic model developed by Zaanen *et al.*[20] and demonstrated in a large number of oxides by Torrance *et al.*[21] and Arima *et al.*[22] Kato *et al.* employed lattice site potential analysis to show that the valence band structure can be tailored by designing the stacking sequence of layers of a number of layered compounds BiOX (X = Cl, Br, I), Bi_4NbO_8X (X = Cl, Br), Bi_2GdO_4X (X = Cl, Br), and $SrBiO_2X$ (X = Cl, Br, I) and therefore, lattice site potential analysis may be useful for designing new photocatalysts.[23] Here we look back at the development of Madelung electrostatic potential and lattice site potential only for perovskite type ABO_3 oxides. We show that the lattice and valence stabilities of perovskite structure type ABO_3 compounds can be understood from simple Madelung electrostatic potential view point and valence stability is directly related to the lattice site potential. Based on the existing literatures, our hypothesis is that the stability and properties of perovskite type ABO_3 oxides can be rationalized better in terms of change in Madelung electrostatic potential energies rather than structural perturbation such as distortions and tolerance factors.[24,25]

The Madelung electrostatic potential and lattice site potentials can be calculated using commercial first principle calculation software packages. We have used freely available software VESTA[10] to recalculate the lattice site potentials and Madelung electrostatic potential directly from the known crystal structures. The Madelung electrostatic potential E_M obtained from VESTA has the unit of MJ mol^{-1} asymmetric unit. In order to compare E_M per mole of each compound with different crystal symmetry (space groups), the E_M output of each compound from VESTA was multiplied by the multiplicity of general Wyckoff position and divided by the number of formula units in the unit cell.

Results and discussion

According to Van Gool and Piken,[6,7] the Madelung electrostatic potential energy E_M can be expressed as

$$E_M(\text{kcal/mol}) = 332 \sum \frac{q_j p_j \phi_j}{2\kappa} \quad (2)$$

where, q_j is total charge number of lattice point j, p_j is frequency of occurrence of j lattice point in the unit cell, ϕ_j is the lattice site potential ($Å^{-1}$) at the lattice point j, and κ is total number of molecules in the unit cell.

The Madelung constant can be expressed as

$$M_a = -a \sum \frac{q_j p_j \phi_j}{2\kappa} \quad (3)$$

where M_a is expressed in terms of the characteristic length a, such as the lattice parameter of unit cell. For compounds with complex structures an arbitrary characteristic length r such as nearest neighbor atomic distance can be defined and the Madelung constant can be expressed as

$$M_r = \frac{r}{a}(M_a) \quad (4)$$

From eqn (2)–(4) the Madelung electrostatic potential can be expressed by

$$E_M = -332 \frac{M_a}{a} = -332 \frac{M_r}{r} \quad (5)$$

In VESTA,[10] lattice site potential ϕ_i and Madelung electrostatic potential E_M of a given structure is calculated using following equations

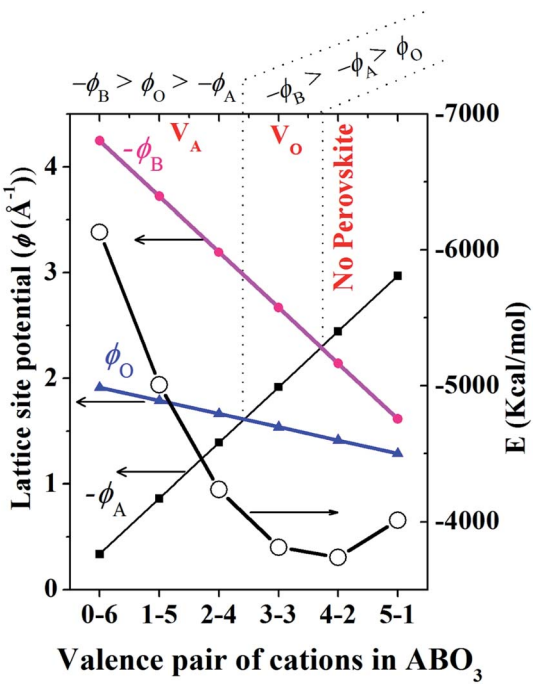

Fig. 2 Variation of lattice site potential and Madelung electrostatic potential energy with varying valence-pair compositions of valences of A and B of perovskite structure type ABO_3 oxides. It should be noted that the sign of ϕ_A and ϕ_B are negative. It was assumed that all the valence pairs have ideal cubic perovskite structure ($a = b = c = 3.881$ Å and $\alpha = \beta = \gamma = 90°$ and space group $Pm\bar{3}m$ (221)).

$$\phi_i = \sum_j \frac{Z_j}{4\pi\varepsilon_0 l_{ij}} \quad (6)$$

where Z_j is valence of ion j, ε_0 is permittivity of vacuum and l_{ij} is distance between ions i and j.

$$E_M = \frac{1}{2}\sum_i \phi_i Z_i W_i \quad (7)$$

where

$$W_i = \frac{(\text{occupancy}) \times (\text{number of equivalent position})}{(\text{number of general equivalent positions})}.$$

For similar structures with fixed atomic position (*e.g.* NaCl, CsCl), the lattice site potential ϕ_j for each site in the crystal structure is inversely proportional to the characteristic length. However, if the characteristic length is fixed, for the first time Yoshimura *et al.*[8] had analyzed that, lattice site potential ϕ_j, the Madelung constant M_a and Madelung electrostatic potential energy E_M varies with the valence states. Fig. 2 shows the relationship between valence state and lattice site potentials ϕ_j as well as Madelung electrostatic potential E_M in ideal cubic perovskite type structure of ABO_3 with fixed lattice constant of 3.881 Å. Based on eqn (5) the Madelung constant M_a also shows similar trend with valence. Fig. 2 shows that the lattice site potential at A site (ϕ_A) and O site (ϕ_O) increase with the valence (0–6), (1–5), (2–4), (3–3) (the first number indicates valence of A and second number indicates valence of B) while the lattice site potential of B ion (ϕ_B) decreases. This re-calculated trend of lattice potential with valence pairs is in excellent agreement with that obtained from method developed by Van Gool and Piken,[6,7] and adapted by Yoshimura *et al.* in 1974.[8] All calculations were performed using VESTA[10] employing the radius of ionic sphere and reciprocal space range of 1.6 Å and 10 $Å^{-1}$,

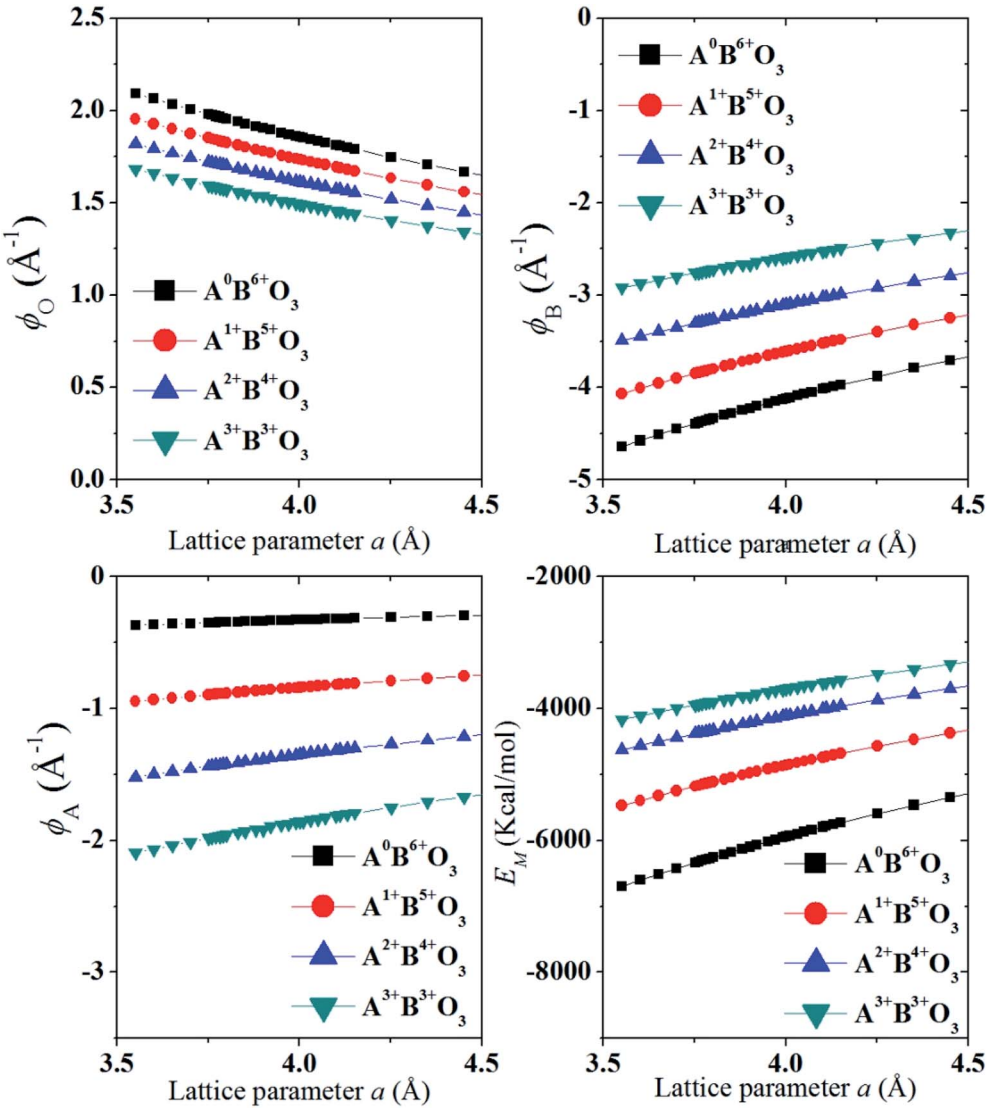

Fig. 3 Variation of lattice site potential of different sites ϕ_A, ϕ_B and ϕ_O and Madelung electrostatic potential E_M, respectively with lattice parameter of different valence pairs $A^0B^{6+}O_3$, (A = Na^0, B = Re^{6+}) as $A^{1+}B^{5+}O_3$, (A = Na^+, B = Ta^{5+}), $A^{2+}B^{4+}O_3$ (A = Sr^{2+}, B = Ti^{4+}) and $A^{3+}B^{3+}O_3$ (A = La^{3+} and B = Al^{3+}) with atomic coordinates of A ($\frac{1}{2}\frac{1}{2}\frac{1}{2}$), B (0 0 0) and O ($\frac{1}{2}$ 0 0) in space group $Pm\bar{3}m$ (221). Radius of ionic sphere and reciprocal space range of 1.6 Å and 10 $Å^{-1}$, respectively.

respectively. For the calculation of ϕ and E_M of $A^0B^{6+}O_3$, a dummy A such as Na atom was placed at $(\frac{1}{2}\ \frac{1}{2}\ \frac{1}{2})$ and B cation Re^{6+} at (0 0 0) atomic coordinates, respectively of space group $Pm\bar{3}m$ (221) with both valence and occupancy, respectively of A were set to zero. The calculation for valence pairs (4–2) and (5–1) assumed hypothetical $A^{4+}B^{2+}O_3$ and $A^{5+}B^{1+}O_3$ perovskite structure type compounds because they rarely exist.

In Fig. 3 we show that, how the lattice site potential (ϕ) of each ionic site and Madelung electrostatic potential (E_M) energy changes with lattice parameter when valence is fixed, for each valence pair in each perovskite structure type ABO_3. The variation observed in Fig. 3 is consistent with the observation of Sabry *et al.* in 2000 (ref. 24). From Fig. 2 and 3 it is observed that lattice site potential for all sites change significantly with valence pairs. Lattice site potential for oxygen in $A^{3+}B^{3+}O_3$ is lowest. Therefore, it can be expected that oxygen can be easily removed from the perovskite type compounds with $A^{3+}B^{3+}O_3$ than $A^{0+}B^{6+}O_3$. Indeed, the occurrence of oxygen vacancy is very common in $A^{3+}B^{3+}O_3$ and this may be of importance during designing catalysts for the availability of active lattice oxygen or designing materials for p- or n- type conductivity.[24,26]

Valence stability is related to lattice energy which mainly arises from Madelung electrostatic potential and more directly related to lattice site potential. We first consider the valence stability of B ions in oxides where both 4+ and 3+ valence state of B ion is known. Example of such B ions are $Ce^{3+/4+}$, $Pr^{3+/4+}$ and $Tb^{3+/4+}$. In order to understand the relative stability of $B^{4+}O_2$ and $B_2{}^{3+}O_3$ we consider the enthalpy change (8) of the decomposition reaction $BO_2 \rightarrow \frac{1}{2}B_2O_3 + \frac{1}{4}O_2$ and corresponding Born–Haber cycle (Scheme 1)

$$\Delta H^* = (UBO_2 - \tfrac{1}{2}UB_2O_3) - I_4 - \tfrac{1}{4}D + \tfrac{1}{2}E \qquad (8)$$

Eqn (8) suggests that high valence of B in oxide BO_2 can be stable if its lattice energy is compensated by other energy terms. Since, the lattice energy is enthalpy at $T = 0$ K ($\Delta H^o = \Delta U^o = \Delta G^o$; the energy terms such as ΔS and RT do not contribute at $T = 0$ K), one can postulate that the stability of high valence ions is enhanced in crystal structure with large lattice energies. A similar analogy can be drawn for the valence stability in complex oxides where multiple ions are present such as in perovskite type ABO_3 compounds. Furthermore, cations provide large electrostatic potential contribution to the total Madelung electrostatic potential in crystal structure as shown in the plots of ϕ_A and ϕ_B in Fig. 3. This is in excellent with the trend of cation site potentials observed by Sabry *et al.*[24] Therefore, the valence stability of cation is rather directly related to the lattice-site potential of the cation site in a crystal structure and the stability enhances when they are present in lattice site with strong lattice site potential such as B site in perovskite structure type ABO_3 oxides.

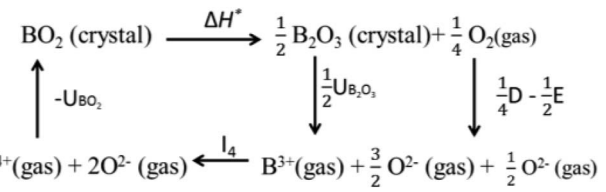

Scheme 1 The Born–Haber cycle of dissociation of BO_2 to B_2O_3. Here, UBO_2 and UB_2O_3 are lattice energies of BO_2 and B_2O_3, respectively. I_4 is ionization energy of B^{3+} to B^{4+}. D and E, respectively are dissociation energy and electron affinity of oxygen.

A number of experimental study has indicated that high valence of some B cation is stable in perovskite type $A^{2+}B^{4+}O_3$ oxides but not in fluorite type $B^{4+}O_2$. For example, investigation on the synthesis of perovskite type ABO_3 compounds had revealed that several stable perovskite type $A^{2+}B^{4+}O_3$ compounds (with A = Ba, Sr and B = Ce, Tb, Pr) can be synthesized and are stable at room temperatures in spite of the poor ambient condition stability of $Pr^{4+}O_2$ and $Tb^{4+}O_2$ and existence of both $Ce_2{}^{3+}O_3$ and $Ce^{4+}O_2$.[27] In order to explain this experimental fact, an in depth analysis of lattice site potential and Madelung site potential was presented in.[8] Here, we have recalculated the lattice site potential and Madelung electrostatic potential using VESTA[10] and presented in Table 1. Our recently calculated values show excellent matches with that using the procedure of Van Gool and Piken.[8] In Table 1 the lattice site potential of A ion in all perovskite structure type compounds appear to be close to those of AO but for B ion, the perovskite structure provides significant lattice site potential gain than that in fluorite structure. Except for $BaTbO_3$ which we believe due to not so accurate estimation of lattice parameter for TbO_2.

Therefore, the experimental observation that B^{4+} was not stable in fluorite structure type $B^{4+}O_2$ but stable in perovskite structure type $A^{2+}B^{4+}O_3$ is in accordance with the data presented in Table 1. The strong lattice site potential at B site results in large total Madelung electrostatic potential of perovskite structure. In general, Fig. 4 shows that lattice site potential of B site is stronger than A or O site in perovskite type ABO_3 in each valence state situation. Therefore, we find that the formation of these perovskite type oxides are associated with significant gain in Madelung electrostatic potential (ΔE_M) calculated by subtracting the combined E_M of rock salt structure type AO and fluorite structure type BO_2 from the E_M of perovskite crystal structure type of final ABO_3 (Table 1). For example, one can reasonably expect that $Ba^{2+}O + Ce^{4+}O_2 \rightarrow Ba^{2+}Ce^{4+}O_3$ reaction may proceed as there is gain in Madelung electrostatic potential ΔE_M of ~ -43 kcal mol^{-1}. It should be noted that this discussion of lattice site potential and Madelung electrostatic potential is first approximation but still can be useful to explain experimental observations. For the calculation of the E_M and ϕ, an ideal cubic structure for ABO_3 has been assumed and all the ions have been considered as point charges. In real crystals however, ions will have certain degree of polarization in their site, and various structural distortion generally leads to the deviation from cubic symmetry of the crystal structure of the perovskites. High structural distortion can lead to the decomposition of ABO_3 to component oxides. Therefore, the practical stability of these perovskite structure type ABO_3 oxides may not be very high.

Table 1 Madelung electrostatic potential energy of some different structured oxides, fluorite (AO_2) rock salt (AO) and perovskite ($A^{2+}B^{4+}O_3$) types. ϕ_A, ϕ_B and ϕ_O are lattice site potentials of A, B and oxygen sites, respectively (see text). The data were calculated using VESTA[10] employing radius of ionic sphere and reciprocal space range of 1.6 Å and 10 $Å^{-1}$, respectively

Compound	Crystal structure	Lattice constant[a] (Å)	Madelung electrostatic potential E_M (kcal mol^{-1})	Difference ΔE_M[b] (kcal mol^{-1})	Lattice site potential ($Å^{-1}$)		
					ϕ_A	ϕ_B	ϕ_O
CeO_2	Fluorite	5.411[a]	−2855.431			−2.801	1.504
PrO_2		5.393[a]	−2864.947			−2.811	1.509
TbO_2		5.22[a]	−2959.725			−2.904	1.559
BaO	NaCl	5.523[a]	−840.791		−1.269		1.269
SrO		5.160[a]	−899.696		−1.358		1.358
$BaCeO_3$	Perovskite	4.396[b]	−3738.779	−42.6	−1.228	−2.822	1.469
$BaPrO_3$		4.372[b]	−3759.255	−53.5	−1.234	−2.837	1.477
$BaTbO_3$		4.280[b]	−3839.885	−39.4	−1.261	−2.898	1.509
$SrCeO_3$		4.291[b]	−3830.060	−74.9	−1.258	−2.890	1.505
$SrPrO_3$		4.280[b]	−3839.885	−75.2	−1.261	−2.898	1.509
$SrTbO_3$		4.186[b]	−3925.916	−66.5	−1.289	−2.963	1.543

[a] Pseudocubic lattice parameters from a: ref. 31 and b: ref. 27. [b] $\Delta E_M = E_M(ABO_3) - [E_M(AO) + E_M(BO_2)]$.

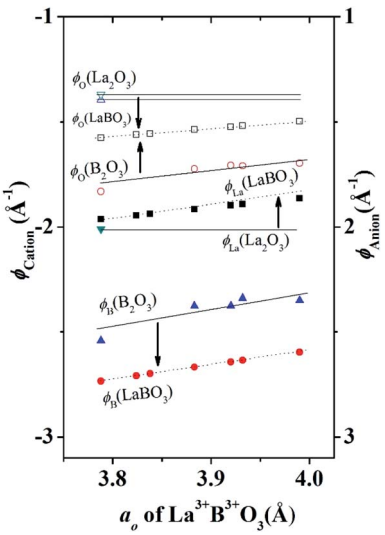

Fig. 4 Variation of lattice site potential ϕ_{La}, ϕ_B and ϕ_O of different sites as a function of pseudocubic lattice parameter (a_o) of several $LaBO_3$ and compared with lattice site potentials of B_2O_3 or La_2O_3. Solid symbols are for cations and hollow symbols are for anion, both dot and solid lines are guide to the eyes.

Takayama-Muromachi *et al.* experimentally obtained change in heat of formation (ΔH_f) for the reaction $A^{2+}O + B^{4+}O_2 \rightarrow A^{2+}B^{4+}O_3$ of several oxides (A = Ca, Sr, Ba, Pb and Cd; B =Ti and Zr).[13] They also calculated change in Madelung electrostatic potential (ΔE_M) from the E_M of $A^{2+}B^{4+}O_3$, AO and BO_2 and showed that heat of formation of perovskite structure type compounds can be written as

$$\Delta H_f \approx \Delta E = \Delta E_M + \Delta E_N \quad (9)$$

It has also been shown that ΔE_M correlates well with Goldschmidt tolerance factor

$$t = \frac{r_A + r_O}{\sqrt{2}\,(r_B + r_O)} \quad (10)$$

(where r_A, r_B and r_O are ionic radius of perovskite structure type ABO_3) and ΔE_M becomes more negative when t reduces from 1 to 0.8. Kamata *et al.* found that lattice site potential for B and Madelung electrostatic potential of $A^{2+}B^{4+}O_3$ (here A = Ca, Sr and Ba and B = Mo), varies linearly with pseudocubic lattice constant and the lattice site potential of Mo is much deeper in perovskite type structure than MoO_2.[28] It is further interesting to note that some of these perovskite-type oxides are so stable that, they are not easily reduced under hydrogen atmosphere at moderate temperatures. From above examples, it can be reasonably hypothesized that the gain in lattice site potential of B site and hence the Madelung electrostatic potential can promote the formation of perovskite structure type ABO_3 compounds. Furthermore, from the lattice site potential consideration, it can be shown that $Ca^{2+}Mn^{4+}O_3$ and $A^{2+}Pb^{4+}O_3$ (A = Ba, Sr) are stable under conditions where the corresponding MnO_2 or PbO_2 decomposes to lower valence oxides.[8]

The valence stabilization due to strong lattice potential at B site as described above for $A^{2+}B^{4+}O_3$ can be further extended to $A^{3+}B^{3+}O_3$. For example, hexagonal structured A_2O_3 (such as La_2O_3) can be reacted with rhombohedral (corundum) structured B_2O_3 (such as Cr_2O_3) or rutile structured BO_2 (such as CrO_2) to form perovskite structure type $A^{3+}B^{3+}O_3$ compounds. However, high valence Ni^{3+} and Co^{3+} in corundum structure Ni_2O_3 and Co_2O_3 respectively are not stable but $LaNi^{3+}O_3$, $LaCo^{3+}O_3$ are stable. Lattice parameters and atomic coordinates for corundum structure Ni_2O_3 and Co_2O_3 is unavailable. In this situation the Madelung electrostatic potential and lattice site potential, can be calculated using a different characteristic length $r = r_B + r_O$ for each known A_2O_3, B_2O_3, BO, BO_2, and ABO_3 using eqn (3)–(5) and graphically estimated for unknown compounds.[8] Further detailed discussion on the characteristic length and Madelung electrostatic potential can be found in.[8,12] However, for comparison purposes, here all lattice site

Table 2 Lattice site potentials and Madelung electrostatic potentials of $LaB^{3+}O_3$, and $B_2{}^{3+}O_3$ compounds calculated using VESTA[10a]

Compound	Structure	Lattice parameter (Å)	Ref[b]	Madelung electrostatic potential E_M (kcal mol^{-1})	Difference ΔE_M (kcal mol^{-1})	Lattice site potential (Å^{-1})		
						ϕ_A	ϕ_B	ϕ_O
La_2O_3	Hexagonal	$a = b = 3.938$, $c = 6.180$, $\alpha = \beta = 90°$, $\gamma = 120°$	i	−3381		−2.0095		1.3945, 1.3687
Al_2O_3	Rhombohedral	$a = b = 4.761$, $c = 12.996$, $\alpha = \beta = 90°$, $\gamma = 120°$	ii	−4352			−2.5402	1.8320
Cr_2O_3		$a = b = 5.07$, $c = 13.872$, $\alpha = \beta = 90°$, $\gamma = 120°$	iii	−4081			−2.3757	1.7241
Fe_2O_3		$a = b = 5.105$, $c = 13.913$, $\alpha = \beta = 90°$, $\gamma = 120°$	iv	−4064			−2.3754	1.7070
Ti_2O_3		$a = b = 5.113$, $c = 13.984$, $\alpha = \beta = 90°$, $\gamma = 120°$	v	−4031			−2.3392	1.7097
V_2O_3		$a = b = 5.126$, $c = 14.134$, $\alpha = \beta = 90°$, $\gamma = 120°$	vi	−4030			−2.3510	1.6972
$LaAlO_3$	Pseudocubic	3.788	vii	−3904	−37	−1.9630	−2.7337	1.5765
$LaCoO_3$		3.824		−3867	—	−1.9446	−2.7081	1.5616
$LaNiO_3$		3.838		−3853	—	−1.9375	−2.6982	1.5559
$LaCrO_3$		3.883		−3808	−77	−1.9152	−2.6670	1.5379
$LaTiO_3$		3.92		−3772	−67	−1.8971	−2.6419	1.5234
$LaFeO_3$		3.932		−3761	−39	−1.8914	−2.6339	1.5188
$LaVO_3$		3.99		−3706	−1	−1.8640	−2.5957	1.4967

[a] ϕ_A, ϕ_B, and ϕ_O are lattice site potentials for A, B and oxygen sites, respectively. [b] References for lattice parameters (i) mp-1968; (ii) COD1000032; (iii) mp-19399; (iv) mp-19770; (v) mp-458; (vi) mp-18937; (vii) F. S. Galasso "Structure, properties and preparation of perovskite type compounds", Pergamon Press, New York (1969); mp stands for materials project, and COD stands for crystallography open database.

potentials were obtained using VESTA[10] that uses eqn (6) and (7) for lattice site potential and Madelung electrostatic potential and presented in Tables 1 and 2. The lattice site potential obtained from compounds with general formula $LaB^{3+}O_3$ (B = Al, Co, Cr, Fe Ni, Ti and V) and $B_2{}^{3+}O_3$ (B = Al, Co, Cr, Fe, Ti and V), are given in Table 2. Fig. 4 shows the gain in lattice site potentials of all the sites in $La^{3+}B^{3+}O_3$. It can be clearly seen that there is significant enhancement of lattice site potential for B site for all $La^{3+}B^{3+}O_3$ from that of corundum structure $B_2{}^{3+}O_3$. Thus, high valence state of Ni and Co is stable in $La^{3+}B^{3+}O_3$ is due to this large lattice site potential at B site and consistent with similar high valence stability situation of $A^{2+}B^{4+}O_3$ as discussed in the previous section. Furthermore, from Fig. 4 it can be stated that the lattice site potential for oxygen is much lower in perovskite structure than corundum structure and therefore, corundum structure of B_2O_3 is more difficult to form oxygen related point defects than perovskite structure type $La^{3+}B^{3+}O_3$. Indeed, a similar analysis has been performed for rutile BO_2 structure as-well[8] and therefore it may be understandable that why oxygen vacancy is rarely seen in rutile or corundum structure although plenty of vacancy present in perovskite structure type $A^{3+}B^{3+}O_3$ compounds. Therefore, lattice site potential analysis provides reasonable understanding of the defect formation in perovskite structure ABO_3 compounds and preparation of many perovskite structure type ABO_3 phases from constituent binary oxides could be understood due to the strong B site potential and gain of Madelung electrostatic potential ΔE_M.

The perovskite structure type compound $A^{4+}B^{2+}O_3$ with valence pair (4–2) cannot be prepared and rarely exist. This can be rationalized from Madelung electrostatic potential view point as well. For example, the calculation of ΔE_M of a hypothetical chemical reaction $ThO_2 + MgO \rightarrow Th^{4+}Mg^{2+}O_3$ revealed that a net Madelung electrostatic potential loss of 184 kcal mol^{-1} (calculated assuming lattice the parameter of $ThMgO_3$ as $a = 4.008$ Å, equivalent to $CaZrO_3$ due to similarity of ionic radius of Ca^{2+} and Th^{4+} as well as Mg^{2+} and Zr^{4+} since the lattice parameter of $ThMgO_3$ is not available) would occur for the formation of perovskite structure type $Th^{4+}Mg^{2+}O_3$.[14] Thus this reaction will not proceed because there is no Madelung electrostatic potential or lattice energy gain in this perovskite type $A^{4+}B^{2+}O_3$ compound and the same hypothesis is applicable to $A^{5+}B^{1+}O_3$. We also note that very recently $A^{4+}B^{2+}O_3$ compounds $Bi^{4+}Ni^{2+}O_3$ and $Pb^{4+}Ni^{2+}O_3$ have been reported to be made only under very high pressure conditions and these can be considered as very special valence combinations where stability is perhaps favored due to other energy factors such as covalency due to hybridization.[29,30]

In Scheme 2 we show similar (see Table 2) calculation of the difference in Madelung electrostatic potential ΔE_M in the preparation of perovskite structure type $EuTiO_3$ from EuO or Eu_2O_3 and TiO_2 or Ti_2O_3. The calculated ΔE_M in Scheme 2

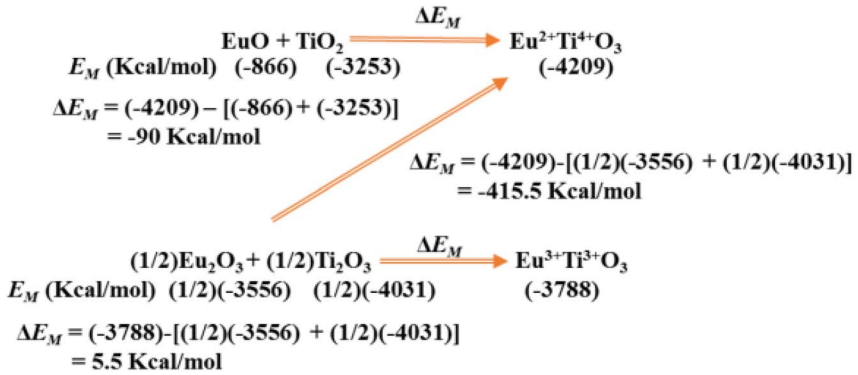

Scheme 2 Change in Madelung electrostatic potential ΔE_M for the formation of $EuTiO_3$. The E_M were calculated using similar conditions as described for other systems using VESTA,[10] assuming perovskite type $Eu^{3+}Ti^{3+}O_3$ and $Eu^{2+}Ti^{4+}O_3$ may have same lattice parameter of 3.904 Å (as the lattice parameter of $Eu^{3+}Ti^{3+}O_3$ is not available).

suggests that $Eu^{2+}Ti^{4+}O_3$ will be more stable than $Eu^{3+}Ti^{3+}O_3$ and usually any preparation will lead to the formation of $Eu^{2+}Ti^{4+}O_3$. This analysis may be expanded to other compounds which are of importance for stabilizing Eu^{2+} at specific ionic sites for the development of visible light emitting phosphor materials.

In conclusion, we have revisited some fundamental aspects of synthesis, stability and properties of perovskite structure type ABO_3. With the use of lattice site potential and Madelung electrostatic potential we have been able to demonstrate that (1) perovskite structure type ABO_3 compounds can be synthesized from their parent binary oxides because of gain in Madelung electrostatic potential which directly correlates with lattice energy, (2) Madelung electrostatic potential and lattice site potentials dictates the stability of perovskite structure and valence stability of cation in perovskite structure is direct consequence of strong cation lattice site potential and (3) the formation of defects such as oxygen vacancy or excess is driven by intrinsic lower lattice site potential of oxygen site. These results (1)–(3) can be seen various experimental data[13,32–34] however, have not been explained in terms of lattice site potential by the authors. Thus, the present article will contribute to understanding of synthesis, structures and properties of functional perovskite type oxides for various areas of applications.

Conflicts of interest

There are no conflicts to declare.

Acknowledgements

The authors are thankful for calculation of some Madelung electrostatic potentials by Dr Alex Lee, and help from profs. Jow-Lay Huang and Jyh-Ming Ting of Department of Materials Science and Engineering of National Cheng Kung University, Tainan, Taiwan. This work was financially supported by the Hierarchical Green-Energy Materials (Hi-GEM) Research Center, from The Featured Areas Research Center Program within the framework of the Higher Education Sprout Project by the Ministry of Education (MOE) and the Ministry of Science and Technology (MOST 110-2634-F-006 -017) in Taiwan.

References

1 V. M. Goldschmidt, *Die Naturwissenschaften*, 1926, **21**, 477–485.
2 K. Zhang, J. Sunarso, Z. Shao, W. Zhou, C. Sun, S. Wang and S. Liu, *RSC Adv.*, 2011, **1**, 1661–1676.
3 Q. Sun and W.-J. Yin, *J. Am. Chem. Soc.*, 2017, **139**, 14905–14908.
4 S. Svarcova, K. Wiik, J. Tolchard, H. J. M. Bouwmeester and T. Grande, *Solid State Ionics*, 2008, **178**, 1787–1791.
5 C. Li, K. C. K. Soh and P. Wu, *J. Alloys Compd.*, 2004, **372**, 40–48.
6 W. Van Gool and A. G. Piken, *J. Mater. Sci.*, 1969, **4**, 95–104.
7 W. Van Gool and A. G. Piken, *J. Mater. Sci.*, 1969, **4**, 105–111.
8 M. Yoshimura, T. Nakamura and T. Sata, *Bull. Tokyo Inst. Technol.*, 1974, **120**, 13–27.
9 R. Roy, *J. Am. Ceram. Soc.*, 1977, **60**, 350–363.
10 K. Momma and F. Izumi, *J. Appl. Crystallogr.*, 2011, **44**, 1272–1276.
11 R. Hoppe, *Z. Naturforsch.*, 1995, **50**, 555–567.
12 L. Glasser, *Inorg. Chem.*, 2012, **51**, 2420–2424.
13 E. Takayama-Muromachi and A. Novartsky, *J. Solid State Chem.*, 1988, **72**, 244–256.
14 T. Ishigaki, Z. S. Nikolic, T. Watanabe, N. Matsushita and M. Yoshimura, *Solid State Ionics*, 2009, **180**, 475–479.
15 J. Shan, Y. Inaguma and M. Itoh, *Solid State Ionics*, 1995, **79**, 245–251.
16 K. Ragavendran, D. Vasudevan, A. Veluchamy and B. Emmanuel, *J. Phys. Chem. B*, 2004, **108**, 16899–16903.
17 N. Ashurov, B. L. Oksengendler, S. Maksimov, S. Rashiodva, A. R. Ishteev, D. S. Saranin, I. N. Burmistrov, D. V. Kuznetsov and A. A. Zakhisov, *Mod. Electron. Mater.*, 2017, **3**(1), 1–25.
18 J. M. Frost, K. T. Butler, F. Brivio, C. H. Hendon, M. V. Schilfgaarde and A. Walsh, *Nano Lett.*, 2014, **14**, 2584–2590.
19 K. Oh-ishi, R. Kobayash and K. Oka, *J. Ceram. Soc. Jpn.*, 2017, **125**(5), 383–386.

20 J. Zaanen, G. A. Sawatzky and J. W. Allen, *Phys. Rev. Lett.*, 1985, **35**(4), 418–421.
21 J. B. Torrance and P. Lacorre, *Physica C*, 1991, **182**, 351–364.
22 T. Arima, Y. Tokura and J. B. Torrance, *Phys. Rev. B: Condens. Matter Mater. Phys.*, 1993, **48**, 17006–17009.
23 D. Kato, K. Hongo, R. Maezono, M. Higashi, H. Kunioku, M. Yabuuchi, H. Suzuki, H. Okajima, C. Zhong, K. Nakano, R. Abe and H. Kageyama, *J. Am. Chem. Soc.*, 2017, **139**(51), 18725–18731.
24 A. Sabry, M. Ayadi and A. Chouikh, *Comput. Mater. Sci.*, 2000, **18**, 345–354.
25 A. Sabry and M. Ayadi, *Int. J. Mod. Phys. C*, 2001, **12**(3), 325–332.
26 E. W. Arnold III and S. Sundaresan, *Chem. Eng. Commun.*, 1987, **58**(1–6), 213–230.
27 M. Yoshimura, T. Nakamura and T. Sata, *Chem. Lett.*, 1973, **2**, 923–928.
28 K. Kamata, T. Nakamura and T. Sata, *Mater. Res. Bull.*, 1975, **10**, 373–378.
29 S. Ishiwata, M. Azuma, M. Takano, E. Nishibori, M. Takata, M. Sakata and K. Kato, *J. Mater. Chem.*, 2002, **12**, 3733–3737.
30 Y. Inaguma, K. Tanaka, T. Tsuchiya, D. Mori, T. Katsumata, T. Ohba, K. Hiraki, T. Takahashi and H. Saitoh, *J. Am. Chem. Soc.*, 2011, **133**(42), 16920–16929.
31 R. W. G. Wycoff, *Crystal structure (II)*, Interscience, New York, 1964.
32 H. Yamamoto, K. Toda, Y. Sakai, T. Nishikubo, I. Yamada, K. Shigematsu, M. Azuma, H. Sagayama, M. Mizumaki, K. Nitta and H. Kimura, *Chem. Mater.*, 2020, **32**, 6892–6897.
33 F. Calle-Vallejo, J. I. Martinez, J. M. Garcia-Lastra, M. Mogensen and J. Rossmeisl, *Angew. Chem., Int. Ed.*, 2010, **49**, 7699–7701.
34 Z. H. Zeng, F. Calle-Vallejo, M. B. Mogensenc and J. Rossmeisl, *Phys. Chem. Chem. Phys.*, 2013, **15**, 7526–7533.